



Sclerochronology and geochemical variation in limpet shells (*Patella vulgata*): A new archive to reconstruct coastal sea surface temperature

Tracy Fenger and Donna Surge

Department of Geological Sciences, University of North Carolina at Chapel Hill, Chapel Hill, North Carolina 27599, USA (donna64@unc.edu)

Bernd Schöne

Department of Paleontology, Increments Research Group, Institute of Geosciences, University of Mainz, Johann-Joachim-Becher-Weg 21, D-55128 Mainz, Germany

Nicky Milner

Department of Archaeology, University of York, The Kings Manor, York YO1 7EP, UK

[1] Climate archives contained in shells of the European limpet, *Patella vulgata*, accumulated in archaeological deposits can potentially provide much needed information about Holocene environmental change in midlatitude coastal areas. Before reconstructing climate information preserved in these zooarchaeological records, we studied the controls on oxygen and carbon isotope ratios ($\delta^{18}\text{O}$ and $\delta^{13}\text{C}$, respectively) in modern specimens. We tested the hypothesis that *P. vulgata* precipitates its shell in isotopic equilibrium with the ambient water by comparing $\delta^{18}\text{O}_{\text{SHELL}}$ with predicted values. Predicted $\delta^{18}\text{O}_{\text{SHELL}}$ was constructed using observed sea surface temperature (SST) records and the equilibrium fractionation equation for calcite and water. We assumed a constant $\delta^{18}\text{O}_{\text{WATER}}$ value of +0.10‰ (VSMOW) based on published regional measurements. Comparison of $\delta^{18}\text{O}_{\text{SHELL}}$ with predicted values revealed that $\delta^{18}\text{O}_{\text{SHELL}}$ values were higher than expected by $+1.01 \pm 0.21\text{‰}$. Consequently, estimated SST calculated from $\delta^{18}\text{O}_{\text{SHELL}}$ was $4.2 \pm 2.3^\circ\text{C}$ lower than observed SST. However, because of the relatively uniform offset between observed and expected $\delta^{18}\text{O}$, an adjustment can be made to account for this predictable vital effect. Thus past climate can be reliably reconstructed using this temperature proxy once the offset is taken into account. $\delta^{13}\text{C}$ values have a similar cyclicity to the $\delta^{18}\text{O}$ variation and therefore vary seasonally. However, $\delta^{13}\text{C}$ is slightly out of phase relative to $\delta^{18}\text{O}$. An overall negative shift in $\delta^{13}\text{C}_{\text{SHELL}}$ over the lifetime of the individual indicates a vital effect associated with ontogeny. Further study of environmental and ecological factors that influence shell $\delta^{13}\text{C}$ is required to evaluate fully the potential of carbon isotope ratios as a useful environmental proxy.

Components: 9679 words, 8 figures, 1 table.

Keywords: gastropoda; oxygen; carbon; climate; temperature proxy.

Index Terms: 4215 Oceanography: General: Climate and interannual variability (1616, 1635, 3305, 3309, 4513); 4825 Oceanography: Biological and Chemical: Geochemistry; 4217 Oceanography: General: Coastal processes; 4227 Oceanography: General: Diurnal, seasonal, and annual cycles (0438); 4870 Oceanography: Biological and Chemical: Stable isotopes (0454, 1041).

Received 21 September 2006; **Revised** 14 March 2007; **Accepted** 11 April 2007; **Published** 4 July 2007.

Fenger, T., D. Surge, B. Schöne, and N. Milner (2007), Sclerochronology and geochemical variation in limpet shells (*Patella vulgata*): A new archive to reconstruct coastal sea surface temperature, *Geochem. Geophys. Geosyst.*, 8, Q07001, doi:10.1029/2006GC001488.

1. Introduction

[2] Coastlines are sensitive to changing climate and environmental conditions, especially sea level fluctuations and storm frequency/intensity. Yet, most of our climate information prior to instrument measurements is reconstructed from deep-sea sediment and terrestrial records [e.g., *Hays et al.*, 1976; *Dansgaard et al.*, 1984; *Oeschger et al.*, 1984; *Huntley and Prentice*, 1988; *Berglund et al.*, 1994; *McManus et al.*, 1994]. Hence a paucity of information exists for coastal areas. Because climate change can have a major impact on human economy, resources, and ecosystems, acquiring proxies from coastal areas for paleoclimate reconstruction is crucial to understanding how coastlines may respond to future climate change.

[3] Using stable isotopes in mollusc shells as proxies for environmental reconstruction began with the observation that most molluscs precipitate their shells in isotopic equilibrium with the ambient water [e.g., *Epstein et al.*, 1951, 1953; *Craig*, 1957; *Grossman and Ku*, 1986]. Later work focused on interpreting the environmental records contained in mollusc shells through a combination of sclerochronology (analysis of growth features formed in accretionary hard parts) and geochemical analyses [e.g., *Jones*, 1983; *Jones et al.*, 1984, 1989; *Jones and Quitmyer*, 1996]. Subsequently, many studies have reconstructed environmental and climate change using carbonate hard parts of aquatic organisms [e.g., *Jones et al.*, 1984; *Krantz et al.*, 1987; *Cohen and Tyson*, 1995; *Elliot et al.*, 2003; *Surge et al.*, 2003; *Schöne and Surge*, 2005; *Surge and Walker*, 2006; *Walker and Surge*, 2006].

[4] Here, we present a new climate archive preserved in shells of the common European limpet, *Patella vulgata*, as variations in oxygen and carbon isotope ratios ($\delta^{18}\text{O}$ and $\delta^{13}\text{C}$, respectively). *P. vulgata* shells are common in coastal Viking deposits (900–1550 AD) in the United Kingdom [Barrett et al., 2004] and potentially record climate change during the Medieval Warm Period and early Little Ice Age. Reconstructing climate from such materials is the next phase of this ongoing work. However, before we can interpret the climate archives contained in archaeological shells, we

must develop proxies using $\delta^{18}\text{O}$ and $\delta^{13}\text{C}$ in modern specimens, which is the aim of this study.

2. Ecology of *Patella vulgata*

[5] *P. vulgata* is a gastropod that inhabits rocky shorelines in the high intertidal and shallow subtidal zones. This species occurs in the cold- and warm-temperate biogeographic provinces from Norway to northern Spain. *P. vulgata* lives in salinities ranging from 20 to 35 psu (practical salinity units) and prior studies document tolerance to extreme atmospheric temperatures ranging from -8.7 to 42.8°C [Crisp, 1965; Branch, 1981], although it precipitates its shell material while submerged across a narrower temperature range. It resides on a home base or scar, and makes short trips away to graze on algae, diatoms, and spores; therefore the shell records environmental conditions from one location.

[6] *P. vulgata* from the United Kingdom slows its growth during the winter, and maximum growth occurs during the early summer [Blackmore, 1969; Lewis and Bowman, 1975; Ekaratne and Crisp, 1982, 1984; Jenkins and Hartnoll, 2001]. Its growth rate contrasts with lower latitude locations, such as the Mediterranean, where other *Patella* species reportedly slow their growth during the summer [Schifano and Censi, 1986]. On the basis of sclerochronology, Ekaratne and Crisp [1984] reported a small slowdown in *P. vulgata* growth during midsummer (July) due to gonad maturation and reproduction, with a second peak in growth rate occurring in late summer (August–September). In contrast, Blackmore [1969] observed that growth continued at its maximal rate until after spawning in the fall. Growth rate varied from approximately 0.005 mm/month to 2.6 mm/month [Blackmore, 1969; Ekaratne and Crisp, 1984]. We used reported growth rates and sclerochronology as guidelines for our microsampling strategy.

3. Study Area

3.1. Shell Collection

[7] In 2000 and 2001, *P. vulgata* specimens were collected alive from St. Mary's Lighthouse, North-

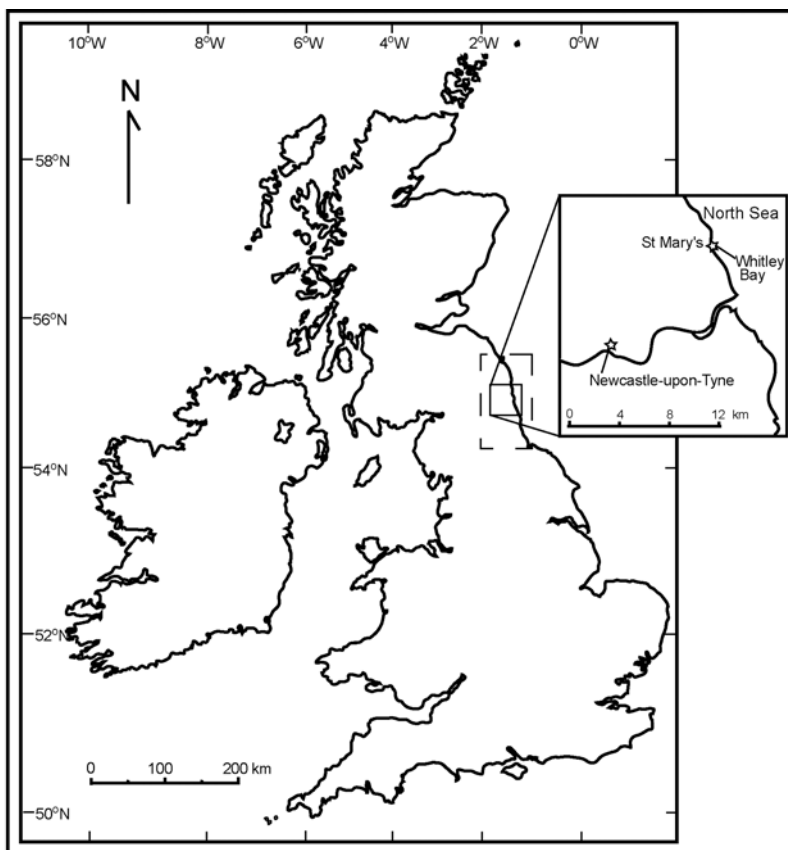


Figure 1. Map of study area at St. Mary's Lighthouse in Whitley Bay, Northumberland, United Kingdom. The major city of Newcastle-upon-Tyne is included for reference. Dashed box indicates location of in situ and satellite SST data and salinity measurements centered around a 1° grid (54.5–55.5°N, 1–2°W). SST data provided by the National Oceanic and Atmospheric Administration (NOAA) Optimum Interpolation (OI) SST V2 database (NOAA-CIRES ESRL/PSD, 2006; <http://www.cdc.noaa.gov>). Salinity data provided by the Centre for Environment, Fisheries, and Aquaculture Science (SAPPHIRE Laboratory Sample Data Management (LSDM) Database, 2006; <http://www.cefas.co.uk>).

umberland, United Kingdom (Figure 1). The site is a natural rock promontory with a tidal causeway that runs out to a lighthouse. Twelve collections of limpets were made from February 2000 to June 2001, and between 25 and 35 limpets were gathered from both high-intertidal and low-intertidal zones midway along the causeway on the southeast side. Individuals were pried off the rocks using a penknife, and the animal was scooped out of the shell by hand at the collection site. The empty shells were taken back to the Bioarchaeology Laboratory at the University of Newcastle and were rinsed clean with warm water. Three high-intertidal zone limpets from the January 2001 (shell NL-0101-2) and June 2001 (shells NL-0601-2 and NL-0601-3) collections were chosen for the isotope analysis presented in this paper.

3.2. Water Properties and Chemistry

[8] Weekly records of sea surface temperature (SST) measured at Newcastle-upon-Tyne, England were obtained from the National Oceanic and Atmospheric Administration (NOAA) Optimum Interpolation (OI) SST V2 database (NOAA-CIRES ESRL/PSD Climate Diagnostics Branch, Boulder, Colorado, 2006; <http://www.cdc.noaa.gov>) (Figure 1). SST ranged from 5.18 to 17.71°C for years 1991 through 2001, with winter temperature averaging $7.13 \pm 0.93^\circ\text{C}$ ($n = 128$) and summer temperature averaging $14.04 \pm 1.56^\circ\text{C}$ ($n = 129$). The NOAA OISST V2 database calculates SST data from a one-degree grid (see Figure 1); therefore the observed SST values were not taken directly from Whitley Bay. This may have resulted in some degree of uncertainty in our comparison. The Centre for Environment, Fisheries and

Aquaculture Science (SAPPHIRE Laboratory Sample Data Management (LSDM) Database, 2006; <http://www.cefas.co.uk>) measured salinity periodically near Whitley Bay, England (54.5–55.5°N, 1–2°W) from 1994 through 1996 (Figure 1). Salinity values ranged from 34.5 to 34.8 psu and averaged 34.6 ± 0.1 psu ($n = 30$), confirming that the *P. vulgata* specimens collected for this study grew under normal marine conditions

(accepted values for normal marine salinity range from 30 to 35 psu) throughout the year.

[9] *Hickson et al.* [1999] measured the oxygen isotope ratio of seawater offshore of Yorkshire, England, southern North Sea. $\delta^{18}\text{O}_{\text{WATER}}$ values averaged $+0.16 \pm 0.04\text{‰}$ (VSMOW) ($n = 8$) in October–November 1994 and $+0.04 \pm 0.03\text{‰}$ (VSMOW) ($n = 3$) in April–July 1997. They calculated an average $\delta^{18}\text{O}_{\text{WATER}}$ value of $+0.10 \pm 0.04\text{‰}$ (VSMOW).

4. Methods

4.1. Analysis of Shell Microstructure

[10] Acetate peels were prepared to (1) identify microstructural layers and growth lines; (2) evaluate preservation of original mineralogy; and (3) distinguish between aragonitic and calcitic mineralogical layers. Shells were sectioned from anterior to posterior, parallel to the maximum growth axis. Cross sections were polished to $1\ \mu\text{m}$ diamond suspension grit (Buehler), and photographed digitally prior to acetate peel preparation (Figure 2a). We prepared acetate peels according to the methods described by *Richardson et al.* [1979] and viewed them under a low-power microscope (2.5x magnification). Polished shell surfaces were immersed in Mutvei's solution to enhance growth lines and increments (see *Schöne et al.* [2005a] for a detailed explanation of this procedure) (Figure 2b). This process allowed us to identify semidiurnal, lunar daily (for an explanation of this term, see *Schöne et al.* [2002]), fortnightly, and annual growth lines and increments, and provided guidelines to determine an appropriate microsampling protocol for geochemical analyses. Feigl's solution was used to verify the location of aragonite and was used in conjunction with microstructure to

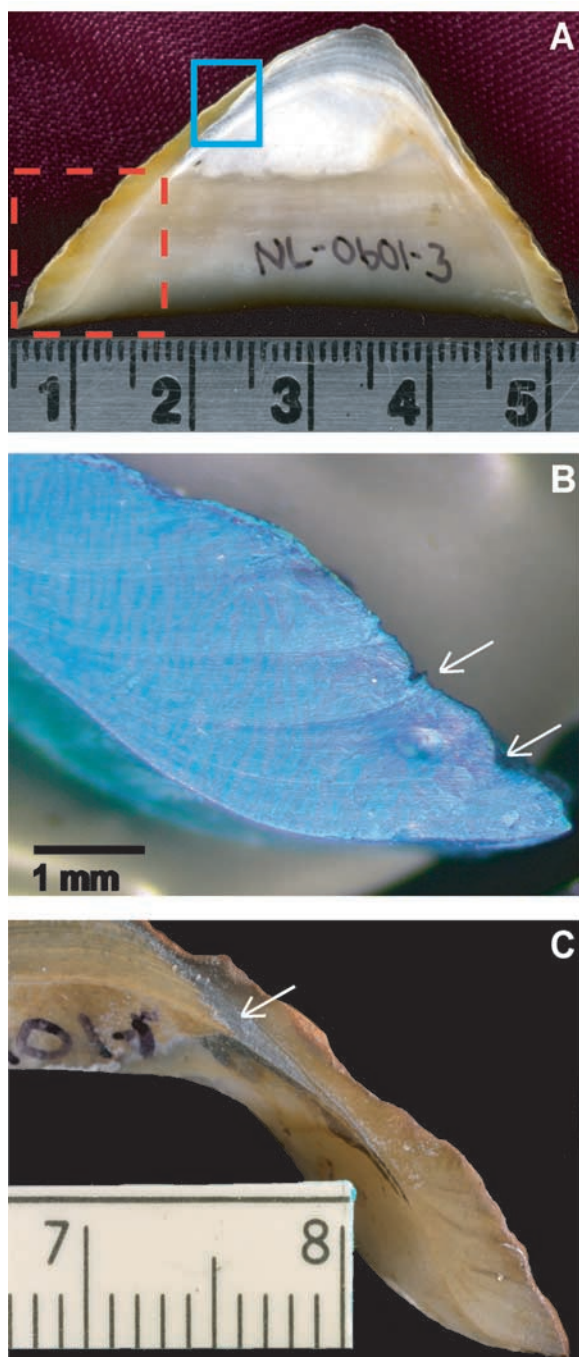


Figure 2. (a) Photograph of polished shell cross section (NL-0601-3). Growth lines are visible on the anterior sagittal section and apex of the sectioned shell. The posterior sagittal section of the shell was sampled along the maximum axis of growth for isotopic analysis. Dashed red square represents the general area of shell sampled for isotopic analysis. Solid blue square represents the shell area depicted in Figure 3. Major units on scale are centimeters. (b) Photograph of shell surface immersed in Mutvei's solution to enhance growth lines and increments (NL-0601-3). White arrows indicate annual growth lines. Scale bar represents 1 mm. (c) Photograph of shell surface stained with Feigl's solution (major units are cm). The areas stained black indicate aragonite (denoted with white arrow).

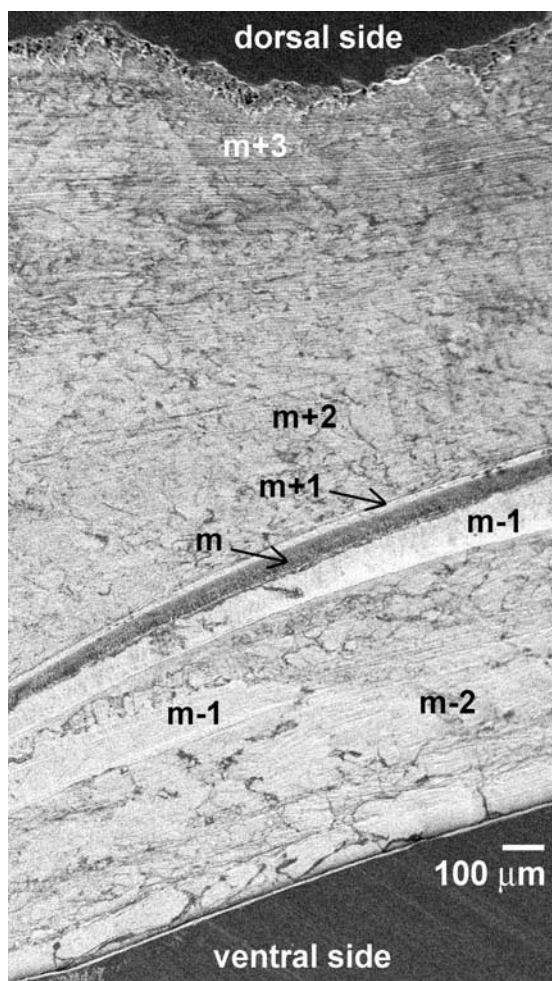


Figure 3. SEM photomicrograph of the shell apex showing the five microstructural layers. The SEM image depicts the same microstructural layers identified in the acetate peels, and a digital photomicrograph was more easily produced from the former. Microstructural layers are labeled according to *MacClintock* [1967], where layers are defined relative to the myostracum (m). Note interlacing relationship between m-2 and m-1 layers. See Figure 2 for general area of shell depicted by SEM photomicrograph. Minor growth lines are also visible in the SEM image.

avoid false positives or false negatives [*Feigl*, 1958] (Figure 2c). *Feigl's* solution is an aqueous solution containing manganese and silver ions and causes a reaction between the manganese and silver ions and the OH⁻ ions produced from calcium carbonate suspended in water. Aragonite shell material is more soluble and reacts more quickly to this solution compared to calcite and consequently, changes to a black color from the reaction. We left our specimen in *Feigl's* solution for 20 minutes. Only if we had left the specimen in

the *Feigl's* solution for a day or two would the calcite stain black and give us a false reading. Hence only the aragonitic portions of the shell stain black. These results allowed us to avoid mixing mineralogy between calcite and aragonite for geochemical analyses.

4.2. Geochemical Analyses

[11] After identifying the microstructural layers, mineralogy, and growth lines, we prepared the shell surfaces for microsampling. Each specimen was set in a metal-based epoxy resin. A 2 mm thick section was cut using a Buehler Isomet low-speed saw, mounted to a glass microscope slide, and repolished. A dental drill system (Minimo micro-mill) attached to a binocular microscope was used to continuously mill out samples, allowing for high-resolution sampling (approximately 50–100 μm spacing). We chose the outer, concentric crossed-foliated and radial, crossed-foliated calcite layers (Figure 3) because (1) the outer aragonite layer in *P. vulgata* is not very extensive [*MacClintock*, 1967] and (2) the inner aragonite and calcite layers are adjacent to the mantle and may be subject to dissolution and resorption during anaerobic conditions [*Lutz and Rhoads*, 1977; *Gordon and Carriker*, 1978; *Signor*, 1982].

[12] Approximately 30–100 μg of carbonate powder were micromilled from each sample path, parallel to growth direction, using a 1 mm drill bit, and sample paths were spaced at 50–100 μm intervals. We collected 117, 108, and 215 samples for δ¹⁸O and δ¹³C analyses from shells NL-0101-2, NL-0601-2, and NL-0601-3, respectively. The samples were reacted with 99% anhydrous phosphoric acid at 72°C in an automated carbonate preparation device (Gas Bench II) coupled to a Finnigan MAT-253 mass spectrometer. Oxygen and carbon isotope ratios of the samples are reported in per mil units (‰) relative to the VPDB carbonate standard. Corrections for ¹⁷O have been made according to *Craig* [1957]. Precision of the instrument determined from replicate analyses was ±0.07‰ for δ¹⁸O and ±0.04‰ for δ¹³C.

[13] Specimen NL-0101-3 was sampled at 70–200 μm intervals for determination of Mg:Ca ratios to assess whether *P. vulgata* shells were composed of low- or high-magnesium calcite (LMC and HMC, respectively). Carbonate samples were dissolved individually in 1.5 mL of dilute Fisher Optima grade HNO₃ + HCl spiked with indium as an internal standard. The solutions were analyzed for Mg and Ca content on a Finnigan *Element*

inductively coupled plasma-mass spectrometer (ICP-MS). It was not possible to accurately weigh the individual samples due to the small sample size; therefore raw solution data (ng/g) are reported as molar Mg:Ca ratios using mmol/mol concentrations. Raw solution data have been converted from molar Mg:Ca ratios to mol-% Mg by calculating the contribution of all measured cations (i.e., Ca, Sr, and Mg) and normalizing to 100%. Check standards and sample replicates and duplicates show an analytical precision better than $\pm 1\%$ RSD (raw standard deviation).

4.3. Predicted Shell $\delta^{18}\text{O}$

[14] To verify agreement with equilibrium precipitation, a predicted shell representing the expected $\delta^{18}\text{O}_{\text{SHELL}}$ precipitated under isotopic equilibrium was calculated using observed weekly SST, $\delta^{18}\text{O}_{\text{WATER}}$ values reported by *Hickson et al.* [1999], and the equilibrium fractionation equation for calcite and water (*Friedman and O'Neil* [1977] modified from *Tarutani et al.* [1969]),

$$1000 \ln \alpha = 2.78 \times 10^6 / T^2 - 2.89 \quad (1)$$

where T is temperature in Kelvin and α is the fractionation factor between calcite and water. We chose the *Friedman and O'Neil* [1977] equation rather than that reported by *Kim and O'Neil* [1997] because the former equation more closely spans the temperature range observed in our study area. This equation was preferred over other linear or quadratic temperature equations derived from species-specific data because no correction is required to adjust the water and carbonate $\delta^{18}\text{O}$ values to the different scales on which they are measured (see *Dettman et al.* [1999, p. 1053] for a more detailed discussion). The term that accounts for mol-% MgCO_3 was omitted because *P. vulgata* secretes a low-Mg calcite shell (see sections 5.4 and 6.2 for further discussion). The relationship between α and δ is

$$\alpha = (\delta_{\text{CALCITE}} + 1000) / (\delta_{\text{WATER}} + 1000) \quad (2)$$

where δ is expressed relative to VSMOW. We assumed a $\delta^{18}\text{O}_{\text{WATER}}$ value of $+0.10\text{‰}$ (see section 3.2). Predicted $\delta^{18}\text{O}$ values calculated from equation (1) were converted from the VSMOW to VPDB scale using the following equation reported by *Coplen et al.* [1983] and *Gonfiantini et al.* [1995]:

$$\delta^{18}\text{O}_{(\text{VPDB})} = (\delta^{18}\text{O}_{(\text{VSMOW})} - 30.91) / 1.03091 \quad (3)$$

[15] To align measured shell $\delta^{18}\text{O}$ with the predicted time series, we assigned calendar dates to the shell isotope record by anchoring the growing edge sample to the shell collection date. This approach was used for specimens NL-0601-2 and NL-0601-3 because both individuals were collected during their growing season in June 2001. In the case of specimen NL-0101-2, because it was collected in January during its period of winter growth retardation, we anchored the growing edge in September of the previous fall before the shell production rate slowed. Our rationale is supported by previous growth studies discussed in the ecology section above. The remaining points were aligned with the predicted time series, taking into consideration ontogeny (e.g., the organism accreted shell more rapidly during juvenile years), annual and fortnightly growth lines identified during the sclerochronologic analysis, and the general pattern of the predicted $\delta^{18}\text{O}$ time series. Shell powder samples were taken at approximately equal distances. This enabled us to calculate the approximate time represented by each sample. In a first approximation, we assumed that the shells grew year-round and thus divided the number of days per year through the number of samples taken between two annual growth lines. This simple assumption, however, is not justified because numerous other studies have demonstrated that most molluscs do not grow all year-round and grow at different rates during different seasons. Thus we used fortnightly and lunar daily growth increments [e.g., *Ekaratne and Crisp*, 1984] for a more precise temporal alignment of the data. Tidal growth patterns turned out to be a useful means to improve the provisional temporal alignment.

5. Results

5.1. Mineralogy and Microstructure

[16] The acetate peels confirmed preservation of original mineralogy and revealed five microstructural shell layers (Figure 3). The two layers interior to the myostracum (muscle attachment site identified by an “m” in Figure 3) are composed of a calcitic, radial crossed-foliated layer (m-2) and an aragonitic, radial crossed-lamellar layer (m-1) (terminology based on *MacClintock* [1967] and *Carter and Hall* [1990]). The three layers exterior to the myostracum are composed of (1) an aragonitic, concentric crossed-lamellar layer (m + 1); (2) a calcitic, concentric crossed-foliated layer (m + 2); and (3) a calcitic, radial crossed-foliated layer (m + 3). Similar to the findings of *MacClintock* [1967],

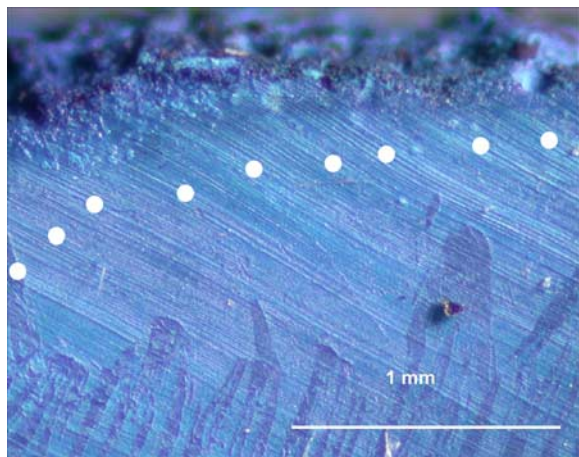


Figure 4. Photomicrograph of shell surface immersed in Mutvei's solution depicting fortnightly, semidiurnal, daily, and lunar growth increments (NL-0601-3). White circles indicate fortnightly bundles composed of semidiurnal and lunar growth increments. Scale bar represents 1 mm.

Feigl's solution revealed that the outer aragonite layer did not occupy a significant portion of the shell. Thus we did not mix calcitic and aragonitic mineralogies while microsampling.

[17] Shell cross sections immersed in Mutvei's solution revealed major and minor growth lines and increments. Major growth lines were identified in the acetate peels, polished shell surfaces, and Mutvei-stained shell sections as thicker, more pronounced lines. Additionally, major growth lines often coincided with an indentation in the outer shell surface (see Figure 2b). Major growth lines, representing interruptions or slowdown in shell growth, were spaced approximately 200 to 2,500 μm apart (Figure 2b). Minor growth increments were approximately 10 to 200 μm in width and consisted of periodic bundles containing 14 to 15 microgrowth increments separated by microgrowth lines (Figure 4). We used the major and minor growth lines and increments to align measured $\delta^{18}\text{O}$ values with the predicted $\delta^{18}\text{O}$ time series.

5.2. Measured Oxygen and Carbon Stable Isotope Ratios

[18] Variation in $\delta^{18}\text{O}$ of all three shells follows a sinusoidal trend (Figure 5) and ranges from +1.07‰ to +2.89‰, +0.85‰ to +3.34‰, and +0.64‰ to +3.44‰ (shells NL-0101-2, NL-0601-2, and NL-0601-3, respectively). $\delta^{18}\text{O}$ values average $+1.93 \pm 0.42\text{‰}$ (NL-0101-2), $+2.02 \pm 0.61\text{‰}$ (NL-0601-2), and $+1.96 \pm 0.75\text{‰}$ (NL-0601-3).

The $\delta^{18}\text{O}$ values of shells NL-0601-2 and NL-0601-3 show similar amplitudes of $\sim 2\text{‰}$. In contrast, shell NL-0101-2 has a diminished range of $\delta^{18}\text{O}$ values ($\sim 1\text{‰}$). Major growth lines identified during the sclerochronologic analysis coincide with the most positive $\delta^{18}\text{O}$ values in all three shells. The major growth lines also correspond with the fewer number of $\delta^{18}\text{O}$ data points representing the most positive $\delta^{18}\text{O}$ values.

[19] Like the $\delta^{18}\text{O}$ values, $\delta^{13}\text{C}$ values of all three shells follow a sinusoidal trend (Figure 5) and range from +0.36‰ to +1.43‰, -0.41‰ to +0.71‰, and -1.54‰ to +0.53‰ (shells NL-0101-2, NL-0601-2, and NL-0601-3, respectively). Variation in $\delta^{13}\text{C}$ averages $+0.99 \pm 0.19\text{‰}$ (NL-0101-2), $+0.25 \pm 0.29\text{‰}$ (NL-0601-2), and $-0.15 \pm 0.45\text{‰}$ (NL-0601-3). Shell NL-0601-3 has the largest range of $\delta^{13}\text{C}$ values compared to the other two shells. $\delta^{13}\text{C}$ in all three shells decreases toward lower values with increasing age (values toward the apex ranged from +0.71‰ to +1.43‰ [NL-0101-2], +0.03‰ to +0.66‰ [NL-0601-2], and -0.30‰ to +0.55‰ [NL-0601-3], whereas near the growing edge values ranged from +0.77‰ to +1.06‰ [NL-0101-2], -0.40‰ to +0.45‰ [NL-0601-2], and -1.28‰ to +0.37‰ [NL-0601-3]). Variation in $\delta^{13}\text{C}$ does not necessarily vary in phase with the oxygen isotope ratios. The $\delta^{13}\text{C}$ values of shells NL-0601-2 and NL-0101-2 occur out of phase with the $\delta^{18}\text{O}$ values. $\delta^{13}\text{C}$ values in shell NL-0601-2 tend to lag behind the $\delta^{18}\text{O}$ values. Conversely, in shell NL-0101-2, $\delta^{13}\text{C}$ values tend to lead ahead of the $\delta^{18}\text{O}$ values. Variation in $\delta^{13}\text{C}$ in shell NL-0601-3 is in phase with the $\delta^{18}\text{O}$ values. However, $\delta^{13}\text{C}$ in the earlier part of shell NL-0601-3 does not exhibit a large range of values; hence $\delta^{13}\text{C}$ does not emulate the full variation of $\delta^{18}\text{O}$. Conversely, in the later part of the shell, the range of $\delta^{13}\text{C}$ values mirrors the range of the $\delta^{18}\text{O}$ values.

[20] The cross-plots of $\delta^{18}\text{O}$ and $\delta^{13}\text{C}$ for all three shells reveal no covariant trend (NL-0101-2: $r^2 = 0.06$, $n = 117$, $p = 0.011$; NL-0601-2: $r^2 = 0.03$, $n = 108$, $p = 0.081$; NL-0601-3: $r^2 = 0.16$, $n = 215$, $p < 0.001$) (Figure 6). However, $\delta^{13}\text{C}$ in the later (more mature) part of shell NL-0601-3 (beginning approximately 3.5 mm from the shell margin) reveals a strong covariant trend with $\delta^{18}\text{O}$ ($r^2 = 0.80$, $n = 90$, $p < 0.001$). Overall, shell NL-0101-2 values do not overlap with the other two shells, with the result that the average $\delta^{13}\text{C}$ value for shell NL-0101-2 is approximately 1‰ more positive than the average $\delta^{13}\text{C}$ values for the two other shells.

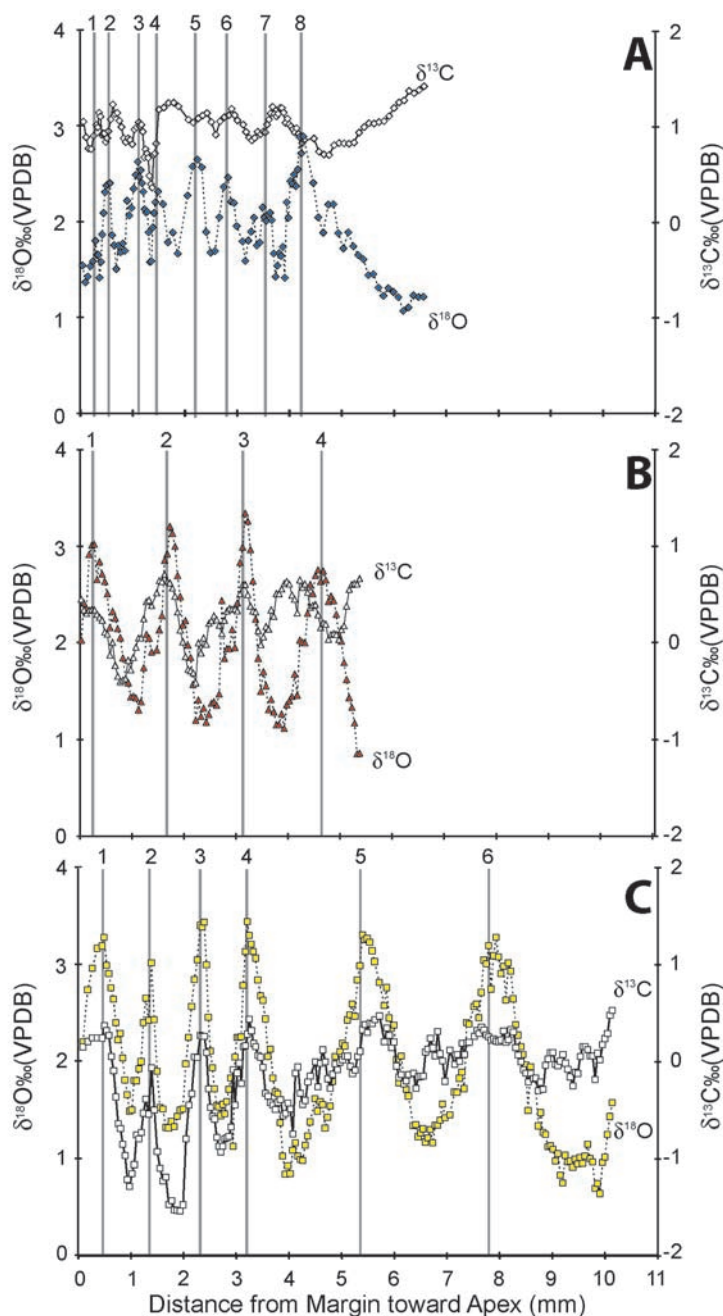


Figure 5. Variation in $\delta^{18}\text{O}$ and $\delta^{13}\text{C}$ versus distance. (a) Shell NL-0101-2, (b) shell NL-0601-2, and (c) shell NL-0601-3. Shells were sampled from the growing edge toward the apex (i.e., age decreases from left to right). Filled symbols represent $\delta^{18}\text{O}$ values, and open symbols represent $\delta^{13}\text{C}$ values (diamonds, NL-0101-2; triangles, NL-0601-2; squares, NL-0601-3). Distance was measured from margin toward the apex (units in mm). Numbered gray vertical lines indicate location of major growth lines.

5.3. Predicted Oxygen Isotope Ratios

[21] The predicted $\delta^{18}\text{O}$ time series is sinusoidal, reflecting the seasonal variation in SST. The time series represents predicted weekly $\delta^{18}\text{O}$ values from 1 July 1991 to 4 June 2001. Predicted $\delta^{18}\text{O}$ values range from -0.37‰ to $+2.41\text{‰}$ and average $+0.96 \pm 0.56\text{‰}$ (Figure 7).

5.4. Mg:Ca Ratios and Mol-% Mg Content

[22] We sampled shell NL-0101-3 incrementally for Mg:Ca ratios to determine whether the calcite was composed of LMC or HMC. Shell NL-0101-3 Mg:Ca ratios range from 13.88 to 16.13. Values of

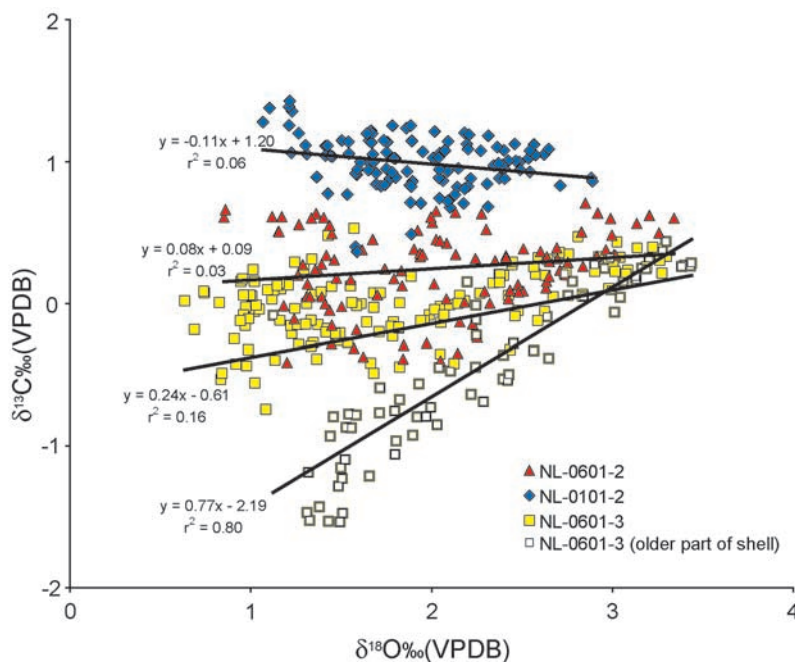


Figure 6. Cross-plot of $\delta^{18}\text{O}$ versus $\delta^{13}\text{C}$ (diamonds, NL-0101-2; triangles, NL-0601-2; squares, NL-0601-3).

mol-% MgCO_3 were calculated and range from 1.39 to 1.59 mol-% Mg (Table 1).

6. Discussion

6.1. Comparison of Measured and Predicted Shell $\delta^{18}\text{O}$

[23] We evaluated (1) whether *P. vulgata* reproduced similar variation in $\delta^{18}\text{O}$ among individuals and (2) whether it precipitates its shell in isotopic equilibrium with the ambient water by comparing measured $\delta^{18}\text{O}$ values against predicted shell values. Specimens NL-0601-2 and NL-0601-3 have similar ranges in $\delta^{18}\text{O}$ values for the period of time where their growth overlaps, with the exception of winter growth during year 4 where specimen NL-0601-2 falls short of NL-0601-3 by 0.69‰ (Figure 5). This exception may reflect a period of slowed growth in shell NL-0601-2 that is not manifested in shell NL-0601-3. See section 6.4 for a detailed discussion on causes of slowed growth. Specimen NL-0101-2 has a more truncated record relative to the other two shells. We attribute this to a slower growth rate in this specimen, which is documented by the number of inferred years relative to distance sampled (NL-0101-2: 8 years, 5.8 mm; NL-0601-2: 4 years, 5.35 mm; NL-0601-3: 6 years, 10.7 mm). These results demonstrate the importance of microsampling multiple shells to ascertain the most complete range of isotopic

variation and to assess whether slowed growth rate resulted in a truncated record.

[24] We compared measured versus predicted values to evaluate isotopic equilibrium. Variation in measured values followed the sinusoidal pattern of the predicted shell; however, measured values were offset positively. The average offset between measured and predicted values was $1.00 \pm 0.21\text{‰}$, $1.02 \pm 0.20\text{‰}$, and $1.03 \pm 0.22\text{‰}$ for shells NL-0101-2, NL-0601-2, and NL-0601-3, respectively, resulting in an overall average offset of $1.01 \pm 0.21\text{‰}$ (Figure 7). Comparison of measured and predicted values also showed that the number of most positive $\delta^{18}\text{O}$ data points are fewer than the number of most negative $\delta^{18}\text{O}$ data points (illustrated by the sharp peaks observed in the $\delta^{18}\text{O}$ profiles in Figure 5), agreeing with previous growth rate observations that *P. vulgata* slows its growth during winter months. These “winter” values represent more time averaging of the shell increments, as compared to amount of time represented by “summer” values. In particular, the range of $\delta^{18}\text{O}$ values in specimen NL-0101-2 does not span the range of predicted $\delta^{18}\text{O}$ values as do the other two specimens, suggesting a relatively slow growth rate in this specimen potentially associated with later ontogeny. This observation agrees with other oxygen isotope studies of mollusc shells, where the truncated range of $\delta^{18}\text{O}_{\text{SHELL}}$ values compared to predicted equilibrium values

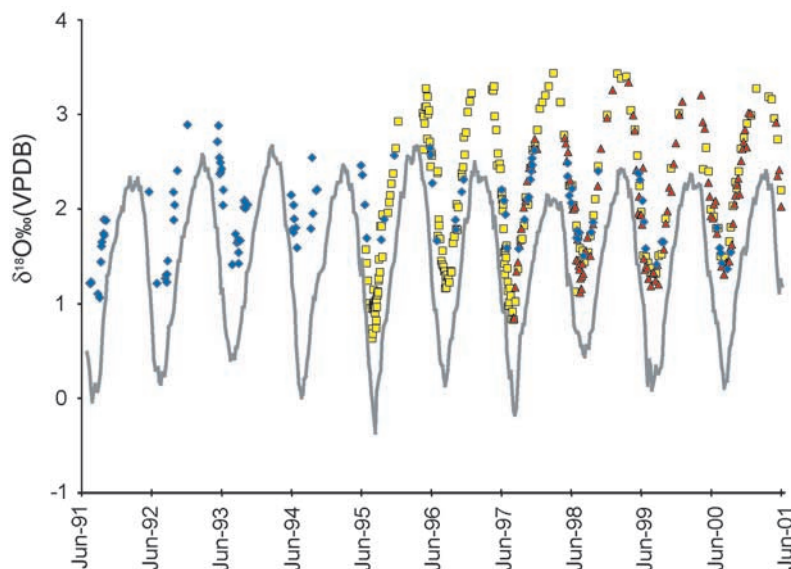


Figure 7. Comparison of predicted versus measured $\delta^{18}\text{O}$. Gray line represents predicted $\delta^{18}\text{O}$. Filled symbols represent measured $\delta^{18}\text{O}_{\text{SHELL}}$ data (diamonds, NL-0101-2; triangles, NL-0601-2; squares, NL-0601-3).

reflected slower growth rate associated with later ontogeny [Jones *et al.*, 1986; Weidman *et al.*, 1994; Goodwin *et al.*, 2003]. An alternative explanation may be that microenvironmental effects cause the diminished range of $\delta^{18}\text{O}_{\text{SHELL}}$ values in NL-0101-2 compared to the other two shells. However, all individuals were collected from the same location on the rocky shore and hence should have experienced the same microenvironmental effects. Moreover, although there was some variability between specimens (i.e., shapes of the $\delta^{18}\text{O}$ curves in Figure 5 and differences in range of values), all three specimens had a relatively consistent offset from predicted values of $1.01 \pm 0.21\text{‰}$, suggesting that factors such as microenvironment do not appear to be the overlying cause for the difference between predicted and measured $\delta^{18}\text{O}$.

[25] To evaluate the effect of the $+1.01\text{‰}$ offset on SST reconstruction, we converted measured $\delta^{18}\text{O}_{\text{SHELL}}$ to estimated SST using the equilibrium fractionation equation (equation (3)), assuming a $\delta^{18}\text{O}_{\text{WATER}}$ value of $+0.10\text{‰}$, and compared estimated SST with observed SST. Without taking the 1.01‰ offset into account, estimated SST averaged $7.9 \pm 2.4^\circ\text{C}$. Observed SST averages $12.08 \pm 2.36^\circ\text{C}$; therefore estimated temperature from $\delta^{18}\text{O}_{\text{SHELL}}$ results in an underestimation of temperature by 4.2°C (Figure 8a). If the offset is taken into account, then corrected SST estimates align with observed SST (Figure 8b). Correction of this offset agrees with previous oxygen isotope studies

on other limpet species, where the authors account for this offset by removing approximately 1‰ from $\delta^{18}\text{O}_{\text{WATER}}$ in their respective paleotemperature equations [Shackleton, 1973; Cohen and Tyson, 1995]. We examined several possible mechanisms to explain the offset from expected equilibrium.

6.2. Mol-% MgCO_3 and Isotopic Disequilibrium

[26] One possible explanation for the positive offset of $\delta^{18}\text{O}$ from equilibrium is that *P. vulgata* shells are composed of HMC. HMC contains greater than 4 mol-% MgCO_3 and is typically ~ 15 mol-% MgCO_3 [Tarutani *et al.*, 1969; Prothero and Schwab, 1996]. The equilibrium fractionation equation for calcite and water must include an additional term of 0.06‰ per mol-% MgCO_3 if the material is HMC [Tarutani *et al.*, 1969; Carpenter *et al.*, 1991]. If the shell is LMC, the equilibrium fractionation equation does not include the mol-% MgCO_3 term. An error can occur in paleotemperature estimates of 0.26°C per mol-% MgCO_3 if the extra term for HMC is not taken into account. If *P. vulgata* shells are composed of HMC, they must contain at least 16 mol-% MgCO_3 to account for the $+1.01 \pm 0.21\text{‰}$ offset from isotopic equilibrium. Shell NL-0101-3 contained 1.39 to 1.59 mol-% MgCO_3 ; therefore calculated paleotemperature estimates would increase by approximately 0.36 to 0.41°C (or a maximum of $+0.10\text{‰}$ shift in predicted $\delta^{18}\text{O}_{\text{SHELL}}$). Thus mol-% MgCO_3

Table 1. Mg:Ca Ratios and mol-% Mg Values for Shell NL-0101-3

Sample	Mg:Ca Ratio	Mol-% Mg
1	14.60	1.44
2	16.07	1.58
3	15.06	1.48
4	14.76	1.45
5	14.45	1.42
6	14.09	1.39
7	13.88	1.37
8	14.51	1.43
9	14.77	1.45
10	14.79	1.46
11	14.83	1.46
12	14.44	1.42
13	15.19	1.49
14	15.48	1.52
15	15.63	1.54
16	15.76	1.55
17	15.91	1.56
18	16.13	1.59
19	15.52	1.53
20	15.16	1.49

does not explain the observed offset from predicted values.

6.3. Vital Effects

[27] Vital effects can cause isotopic disequilibrium in carbonate skeletons. Organisms that display vital effects, where observed $\delta^{18}\text{O}$ values are more positive than expected equilibrium values, include barnacles, foraminifera, benthic calcareous algae, ahermatypic corals, and marine snails [Land *et al.*, 1977; Wefer and Berger, 1980, 1981, 1991; Wefer and Killingley, 1980; Killingley and Newman, 1982; Smith *et al.*, 1988]. In the case of barnacles and marine snails, both are intertidal organisms with sessile life habits similar to limpets; therefore life habit may explain the similar positive offset from expected equilibrium. However, Schöne *et al.* [2007] did not observe any offset from expected $\delta^{18}\text{O}$ in marine intertidal and shallow marine snails from the North Sea. Apparently, disequilibrium fractionation may not depend on a specific taxonomic rank, but rather occurs in some species and not in others. The underlying cause for this similar positive offset from expected equilibrium may relate to similar processes of shell precipitation.

[28] Shell precipitation in molluscs occurs within the extrapallial fluid (EPF), located between the mantle and shell. Oxygen and carbon arrive at the biomineralization site for carbonate precipitation through ion sources involving (1) CO_2 diffusing

through the mantle cavity or (2) HCO_3^- and CO_3^{2-} moving actively across the mantle epithelium [Wheeler, 1992]. Departures from isotopic equilibrium, classified as kinetic or metabolic isotope effects, potentially result from processes affecting these ion sources.

[29] Kinetic isotope effects involve CO_2 hydration and hydroxylation processes, where the slow reaction rate of the heavier ^{18}O and ^{13}C isotopes preferentially incorporates the lighter isotopes into the biomineralization medium (e.g., EPF in molluscs or extracytoplasmic calcifying fluid in corals) [McConnaughey, 1989a, 1989b]. Kinetic isotope effects cause the depletion of both ^{18}O and ^{13}C relative to equilibrium values, with increased growth rates causing further depletion of ^{18}O and ^{13}C [Erez, 1978; McConnaughey, 1989b]. However, there is no correlation between $\delta^{18}\text{O}$ and $\delta^{13}\text{C}$ in all three limpet shells, suggesting that kinetic isotope effects are minimal for *P. vulgata*, with the exception of the later part of shell NL-0601-3 (Figure 5) [McConnaughey, 1989b; Spero *et al.*, 1997; Elliot *et al.*, 2003]. The older (more mature) part of shell NL-0601-3 exhibits a strong covariant trend between $\delta^{13}\text{C}$ and $\delta^{18}\text{O}$, which is consistent with observations from previous studies [e.g., Erez, 1978; McConnaughey, 1989a, 1989b; Smith *et al.*, 2000].

[30] Metabolic isotope effects due to incorporation of respired CO_2 [Swart, 1983] or changes in pH [McConnaughey, 1989b] could potentially apply to ^{18}O and ^{13}C enrichment relative to equilibrium. However, many studies invoke mechanisms to explain observed depletions of ^{18}O and ^{13}C [e.g., McCrea, 1950; Erez, 1978; Swart, 1983; McConnaughey, 1989a, 1989b; Usdowski and Hoefs, 1993; Spero and Lea, 1996; Spero *et al.*, 1997; Zeebe, 1999; Smith *et al.*, 2000; Adkins *et al.*, 2003]. Alternatively, McConnaughey [1989a] suggested that the enrichment of ^{18}O in barnacle calcite relative to calcite equilibrium does not fall under kinetic or metabolic disequilibrium and may represent some other form of disequilibrium (i.e., some unknown phenomenon). This may be the same for our limpet specimens. Hence other studies have attempted to explain enrichment of ^{18}O relative to equilibrium with other external or internal processes.

[31] Schifano and Censi's [1983] study of oxygen isotope ratios in *Patella coerulea* shells attributed ^{18}O enrichment to precipitation during evaporative conditions (i.e., an external process) within and around the shell at intermediate tide. If the limpets

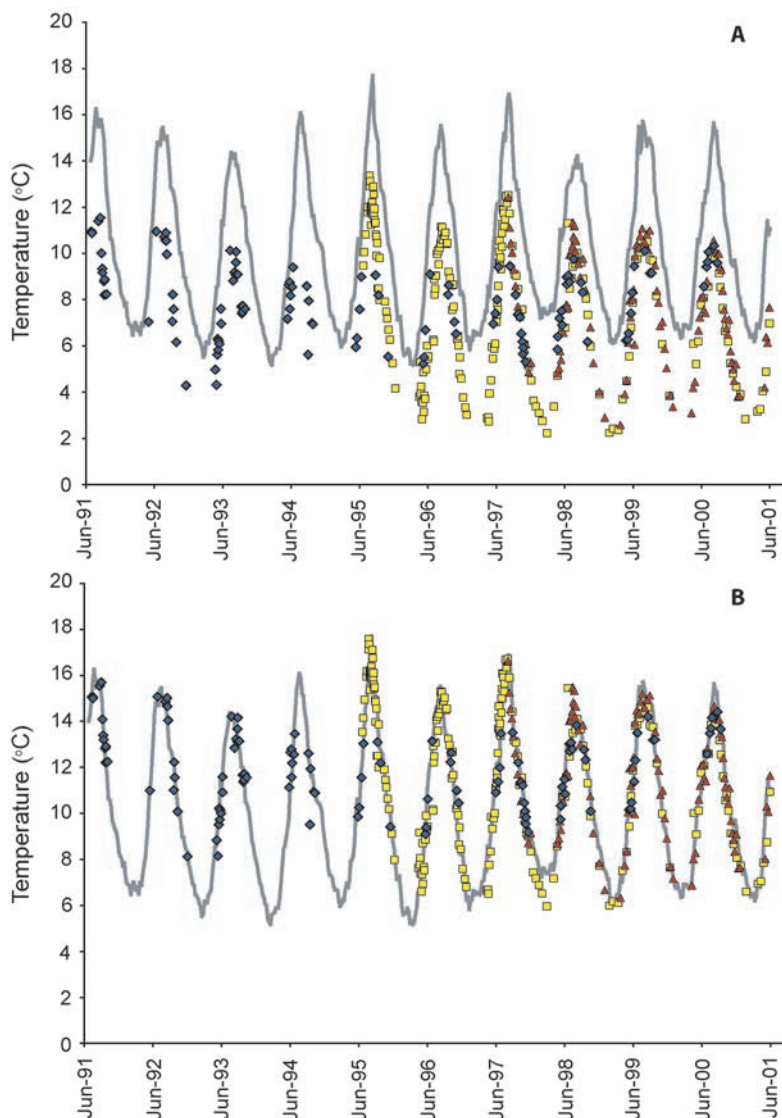


Figure 8. Comparison of observed and estimated SST. Gray line represents observed SST. Filled symbols represent estimated SST from $\delta^{18}\text{O}_{\text{SHELL}}$ (diamonds, NL-0101-2; triangles, NL-0601-2; squares, NL-0601-3). (a) Time series of observed and estimated SST. (b) Time series of observed SST and corrected estimated SST. Subtracting 1.51‰ from $\delta^{18}\text{O}_{\text{SHELL}}$ of the equilibrium fractionation equation results in an agreement between estimated SST and the observed record.

lived where microhabitat conditions influenced $\delta^{18}\text{O}_{\text{WATER}}$, such as tide pools, then this idea could possibly explain the ^{18}O enrichment. However, a subsequent study by *Schifano and Censi* [1986] using subtidal *P. coerulea* observed similar departures from isotopic equilibrium, suggesting that evaporation may not control the disequilibrium. Moreover, our limpet specimens were not collected from tide pools. Conversely, other studies observed desiccation stress as a significant factor in limpet biology [Davies, 1969; Branch, 1981; Verderber et al., 1982; Lowell, 1984]. In particular, Davies

[1969] noted a lag time where limpets come back to osmotic equilibrium after being emerged. If desiccation stress is important to the organism, then the evaporation of seawater associated with desiccation could potentially influence $\delta^{18}\text{O}_{\text{SHELL}}$. However, evaporation would likely cause a variable offset in the oxygen isotope ratios whenever the organism accretes new shell material (i.e., evaporation affects the oxygen isotope composition of the seawater and hence the isotopic composition of the shell). Because we found a consistent offset from equilibrium values, evaporation does not

likely explain the $\delta^{18}\text{O}$ disequilibrium in limpet shells.

[32] Alternatively, an internal process may contribute to the transport of ^{16}O isotopes out of the calcifying medium. Land et al. [1977] attributed shell ^{18}O enrichment relative to equilibrium in ahermatypic, scleractinian corals to active water transport across membrane surfaces through the coelenteron or active formation (and translocation) of organic intermediates. Perhaps similar internal processes create the ^{18}O enrichment in *P. vulgata* shells relative to equilibrium.

[33] In summary, understanding the mechanism responsible for ^{18}O enrichment relative to calcite equilibrium in shells of *P. vulgata* warrants further study. Measuring *P. vulgata* EPF may provide some additional insight into the calcification medium and process, as well as obtaining detailed $\delta^{18}\text{O}_{\text{WATER}}$ data to assess local seawater conditions. Furthermore, a latitudinal comparison of *P. vulgata* may help test whether the offset from isotopic equilibrium relates to differences in temperature and growth rate processes at different latitudes. Although $\delta^{18}\text{O}$ of *P. vulgata* shells is not in equilibrium with expected values, the predictable and relatively uniform offset suggests $\delta^{18}\text{O}_{\text{SHELL}}$ can be reliably used to reconstruct SST once this offset is taken into account.

6.4. Timing of Growth Line Formation

[34] Sclerochronologic studies of mollusc shells have attributed the formation of annual growth lines to a variety of causes, including minimum or maximum temperatures, reproductive processes (i.e., spawning), and food supply [e.g., Pannella and MacClintock, 1968; Lutz and Rhoads, 1977; Jones, 1983; Arthur and Allard, 1987; Jones et al., 1989, 1990; Cerrato et al., 1991; Jones and Quitmyer, 1996; Surge et al., 2001; Schöne et al., 2005b]. In this study, the major growth lines (i.e., the largest and most pronounced growth lines visible on the shell surfaces; Figure 2) identified during sclerochronologic analysis correspond to the most positive $\delta^{18}\text{O}$ values (Figure 5), suggesting the major growth lines are annual and formed during winter. Shells contain fewer measured $\delta^{18}\text{O}$ values corresponding to the cold season, further supporting the observation that growth rate slows down during winter months. Our observation agrees with growth rate studies of *P. vulgata* from the United Kingdom, which have revealed decreased growth rate during winter [Blackmore, 1969; Lewis and Bowman, 1975; Ekaratne and

Crisp, 1984; Jenkins and Hartnoll, 2001]. SST dropping below the optimal growth temperature ($12\text{--}17^\circ\text{C}$ based on growth rate observations by Ekaratne and Crisp [1984]) or reproductive processes (i.e., spawning occurring in early fall [Blackmore, 1969; Branch, 1981]) may cause this slowdown or cessation in growth.

[35] The major growth line observations of *P. vulgata* agree with other midlatitude to high-latitude sclerochronologic studies of other molluscan species. For example, sclerochronologic studies of the bivalves, *Mercenaria mercenaria*, *Spisula solidissima*, and *Arctica islandica*, all reported growth slowdown during winter due to cold temperatures, as well as potential slowdown during fall caused by spawning and winter caused by food shortage [Pannella and MacClintock, 1968; Jones, 1980; Williams et al., 1982; Arthur and Allard, 1987; Jones et al., 1989; Weidman et al., 1994; Schöne et al., 2005b]. Similarly, growth rate in other phyla from midlatitudes to high latitudes, such as sub-arctic to arctic barnacles (*Balanus balanoides*) and temperate fishes (*Encrasicholina punctifer*) (growth rate determined from the otoliths or ear bones), decreases during winter, related to temperature and reproductive processes [Bourget, 1980; Pannella, 1980; Wang and Tzeng, 1999]. These same processes likely contribute to the reduced growth rate of *P. vulgata* during winter.

[36] Blackmore [1969] reported mean monthly growth rates for *P. vulgata* ranging from approximately 0.12 to 1.5 mm/month (which potentially equates to 1.44 to 18 mm/year). In contrast, Jenkins and Hartnoll [2001] observed annual growth rates for sheltered and exposed shore *P. vulgata* ranging from 2 to 4.4 mm/year. Annual growth rates from our Whitley Bay specimens range from approximately 0.2 mm to 2.5 mm/year, agreeing more closely with Jenkins and Hartnoll's [2001] observations. A number of factors may explain the slower growth observed in the Whitley Bay specimens: (1) local temperature in the study area; (2) position on the shoreline (e.g., our specimens were collected from the high intertidal zone where they are not completely submerged at all times); and (3) ontogeny (i.e., our specimens may have been older compared to these other studies). However, the combination of sclerochronology and oxygen isotope analysis suggests that the major growth lines observed do indeed represent annual increments of growth.

[37] Minor growth increments identified during sclerochronologic analysis are arranged in periodic

bundles containing approximately 14 to 15 micro-growth increments (Figure 4), suggesting that the minor growth increments represent fortnights, composed of semidiurnal and lunar daily micro-growth increments controlled by tides. Previous growth rate studies of *P. vulgata* observed these minor fortnightly and daily growth increments [Ekaratne and Crisp, 1982, 1984], and sclerochronologic studies of other gastropods reported similar findings [e.g., Schöne et al., 2007]. Moreover, other studies have observed tidally controlled growth patterns in shells of different molluscan species [e.g., Pannella and MacClintock, 1968; Evans, 1972; Clark, 1974; Goodwin et al., 2001; Schöne et al., 2007], which are in accordance with our observations. The underlying reason for tidally controlled shell growth may lie in changes in hydrodynamic activity, temperature and, most likely, food supply. In fact, the foraging activity of *P. vulgata* closely coincides with the tides. Continuous automatic in-situ recordings revealed that greatest feeding activity occurs during nocturnal low tides, while most reduced activity is associated with spring tides [Santina et al., 1994]. Feeding and shell growth are intimately linked with each other and thus further substantiate our and previous workers' findings on tidally controlled microincrement widths.

6.5. Variability in Shell $\delta^{13}\text{C}$

[38] Unlike measured $\delta^{18}\text{O}$, $\delta^{13}\text{C}$ is more difficult to interpret because we lack the appropriate water property data (e.g., chlorophyll *a* (a proxy for primary productivity), $\delta^{13}\text{C}$ of dissolved inorganic carbon (DIC), pH, etc.). However, because variation in $\delta^{13}\text{C}$ has a similar cyclicity to $\delta^{18}\text{O}$, we infer a seasonal influence on its variability. Some studies have found seasonal variation in $\delta^{13}\text{C}$ corresponding to changes in salinity [e.g., Surge et al., 2001; Fry, 2002]; however, salinity in our study area remains near normal marine values throughout the year. Conversely, other studies correlate seasonal variation in $\delta^{13}\text{C}$ with DIC of seawater mediated by primary productivity and decay of organic matter [e.g., Arthur et al., 1983; Krantz et al., 1987; Hickson et al., 1999; Schöne et al., 2005b].

[39] In the later part of shell NL-0601-3, the correlation between $\delta^{13}\text{C}$ and $\delta^{18}\text{O}$ suggests vital effects may influence $\delta^{13}\text{C}$ values. The lack of reproducibility in $\delta^{13}\text{C}$ among shells lends support to the influence of vital effects. Like the $\delta^{18}\text{O}$ values, $\delta^{13}\text{C}$ values of shell NL-0101-2 have a

diminished amplitude relative to the two other shells, possibly relating to vital effects associated with ontogenetic change. Decreasing $\delta^{13}\text{C}$ values in all three shells as age increases may also relate to ontogenetic changes, which other studies have attributed to increased metabolic CO_2 intake [e.g., Krantz et al., 1987; Klein et al., 1996; Elliot et al., 2003; Lorrain et al., 2004]. Although $\delta^{13}\text{C}$ from shell NL-0601-3 varies simultaneously with $\delta^{18}\text{O}$, there is a lag between $\delta^{13}\text{C}$ and $\delta^{18}\text{O}$ values of shells NL-0601-2 and NL-0101-2. Reasons for this time lag are unknown. Comparison of $\delta^{13}\text{C}_{\text{SHELL}}$ with pH, $\delta^{13}\text{C}_{\text{DIC}}$, CO_2 or chlorophyll *a* concentration may help decipher the processes governing $\delta^{13}\text{C}$ in all three shells.

7. Conclusions

[40] Combining sclerochronology and oxygen isotope analysis in *P. vulgata* shells allowed us to develop a new archive to reconstruct coastal environmental conditions in midlatitudes to high latitudes in the eastern North Atlantic. Identification of major growth lines on the shell surfaces coincide with the most positive oxygen isotope ratios suggesting the growth lines form annually during winter and represent slowdown or cessation of growth. Our hypothesis that *P. vulgata* precipitates its shell in isotopic equilibrium with ambient water was tested by comparing measured shell $\delta^{18}\text{O}$ with predicted $\delta^{18}\text{O}$. We found that $\delta^{18}\text{O}_{\text{SHELL}}$ values are $1.01 \pm 0.21\text{‰}$ more positive than predicted values and SST was underestimated by $\sim 4^\circ\text{C}$ compared to observed SST. However, this offset from isotopic equilibrium is predictable and therefore can be taken into account by subtracting 1.01‰ from $\delta^{18}\text{O}_{\text{SHELL}}$ in the equilibrium fractionation equation for calcite and water [Tarutani et al., 1969; Friedman and O'Neil, 1977]. Other factors, such as mol-% Mg content, were considered, but ruled out. We conclude that $\delta^{18}\text{O}_{\text{SHELL}}$ is a valuable proxy for climate reconstruction.

[41] We were unable to compare $\delta^{13}\text{C}_{\text{SHELL}}$ with local $\delta^{13}\text{C}_{\text{DIC}}$, pH, CO_2 , or primary productivity records, but the similar cyclicity of $\delta^{18}\text{O}$ and $\delta^{13}\text{C}$ shell values suggests that seasonal processes influence variation in $\delta^{13}\text{C}_{\text{SHELL}}$. Changes in the amplitude and trend of $\delta^{13}\text{C}$ over the lifetime of the individual suggest that vital effects and ontogeny may influence $\delta^{13}\text{C}$ values. Further study may find $\delta^{13}\text{C}_{\text{SHELL}}$ in *P. vulgata* a useful proxy for environmental and ecological change.

Acknowledgments

[42] Thanks to Joe Carter, Laurie Steponaitis, Kacey Lohmann, David Dettman, and Ethan Grossman for contributing to the quality of this paper through comments and discussions. The reviews of Andrew Johnson and an anonymous reviewer greatly improved this manuscript. Scott Carpenter provided invaluable help and insight during the early stages of this project. Ted Huston performed Mg:Ca analyses at the Keck Elemental Geochemistry Laboratory, University of Michigan. Partial funding was provided by the National Science Foundation (0318152) and the American Chemical Society's Petroleum Research Fund (39318-G2), both awarded to D.S., and a Geological Society of America graduate research grant (7947-05) and Sigma Xi Research Society Grant-In-Aid of Research, both awarded to T.F.

References

- Adkins, J. F., E. A. Boyle, W. B. Curry, and A. Luttringer (2003), Stable isotopes in deep-sea corals and a new mechanism for "vital effects", *Geochim. Cosmochim. Acta*, *67*, 1129–1143.
- Arthur, M. A., and D. J. Allard (1987), Unlocking the mysteries of *Mercenaria*, *Maritimes*, *31*, 14–17.
- Arthur, M. A., D. F. Williams, and D. S. Jones (1983), Seasonal temperature-salinity changes and thermocline development in the mid-Atlantic Bight as recorded by the isotopic composition of bivalves, *Geology*, *11*, 655–659.
- Barrett, J. H., A. M. Locker, and C. M. Roberts (2004), The origins of intensive marine fishing in medieval Europe: The English evidence, *Proc. R. Soc. London, Ser. A*, *271*, 2417–2421.
- Berglund, B. E., S. Björck, G. Lendahl, H. Bergsten, K. Nordberg, and E. Kolstrup (1994), Late Weichselian and environmental change in southern Sweden and Denmark, *J. Quat. Sci.*, *9*, 127–132.
- Blackmore, D. T. (1969), Studies of *Patella vulgata* L.I. Growth, reproduction, and zonal distribution, *J. Exp. Mar. Biol. Ecol.*, *3*, 200–213.
- Bourget, E. (1980), Barnacle shell growth and its relationship to environmental factors, in *Skeletal Growth of Aquatic Organisms: Biological Records of Environmental Change*, edited by D. C. Rhoads and R. A. Lutz, pp. 469–491, Springer, New York.
- Branch, G. M. (1981), The biology of limpets: Physical factors, energy flow, and ecological interactions, *Oceanogr. Mar. Biol. Ann. Rev.*, *19*, 235–280.
- Carpenter, S. J., K. C. Lohmann, P. Holden, L. M. Walter, T. J. Huston, and A. N. Halliday (1991), $\delta^{18}\text{O}$ values, $^{87}\text{Sr}/^{86}\text{Sr}$ and Sr/Mg ratios of Late Devonian abiotic marine calcite: Implications for the composition of ancient seawater, *Geochim. Cosmochim. Acta*, *55*, 1991–2010.
- Carter, J. G., and R. M. Hall (1990), Polyplacophora, Scaphopoda, Archaeogastropoda and Paragastropoda (Mollusca), in *Skeletal Biomineralization: Patterns, Processes and Evolutionary Trends*, vol. 2, edited by J. G. Carter, pp. 29–51, Van Nostrand Reinhold, Hoboken, N. J.
- Cerrato, R. M., H. V. E. Wallace, and K. G. Lightfoot (1991), Tidal and seasonal patterns in the chondrophore of the soft-shell clam *Mya arenaria*, *Biol. Bull. (Woods Hole)*, *181*, 307–311.
- Clark, G. R. II (1974), Growth line in invertebrate skeletons, *Annu. Rev. Earth Planet. Sci.*, *2*, 77–99.
- Cohen, A. L., and P. D. Tyson (1995), Sea-surface temperature fluctuations during the Holocene off the south coast of Africa: Implications for terrestrial climate and rainfall, *Holocene*, *5*, 304–312.
- Coplen, T. B., C. Kendall, and J. Hopple (1983), Comparison of stable isotope reference samples, *Nature*, *306*, 236–238.
- Craig, H. (1957), Isotopic standards for carbon and oxygen and correction factors for mass-spectrometric analysis of carbon dioxide, *Geochim. Cosmochim. Acta*, *12*, 133–149.
- Crisp, D. J. (1965), Observations on the effect of climate and weather on marine communities, in *The Biological Significance of Climatic Changes in Britain*, edited by C. G. Johnson and L. P. Smith, pp. 63–77, Elsevier, New York.
- Dansgaard, W., S. J. Johnsen, H. B. Clausen, D. Dahl-Jensen, N. Gundestrup, and C. U. Hammer (1984), North Atlantic climatic oscillations revealed by deep Greenland ice cores, *Geophys. Monogr.*, *29*, 288–298.
- Davies, P. S. (1969), Physiological ecology of *Patella*. III. Desiccation effects, *J. Mar. Biol. Assoc. U.K.*, *49*, 291–304.
- Dettman, D. L., A. K. Reische, and K. C. Lohmann (1999), Controls on the stable isotope composition of seasonal growth bands in aragonitic freshwater bivalves (unionidae), *Geochim. Cosmochim. Acta*, *63*, 1049–1057.
- Ekaratne, S. U. K., and D. J. Crisp (1982), Tidal micro-growth bands in intertidal gastropod shells, with an evaluation of band-dating techniques, *Proc. R. Soc. London, Ser. B*, *214*, 305–323.
- Ekaratne, S. U. K., and D. J. Crisp (1984), Seasonal growth studies of intertidal gastropods from shell micro-growth band measurements, including a comparison with alternative methods, *J. Mar. Biol. Assoc. U.K.*, *64*, 13–210.
- Elliot, M., P. B. deMenocal, B. K. Linsley, and S. S. Howe (2003), Environmental controls on the stable isotopic composition of *Mercenaria mercenaria*: Potential application to paleoenvironmental studies, *Geochem. Geophys. Geosyst.*, *4*(7), 1056, doi:10.1029/2002GC000425.
- Epstein, S., R. Buchsbaum, H. Lowenstam, and H. C. Urey (1951), Carbonate-water isotopic temperature scale, *Geol. Soc. Am. Bull.*, *62*, 417–425.
- Epstein, S., R. Buchsbaum, H. A. Lowenstam, and H. C. Urey (1953), Revised carbonate-water isotopic temperature scale, *Geol. Soc. Am. Bull.*, *64*, 1315–1326.
- Erez, J. (1978), Vital effect on stable-isotope composition seen in foraminifera and coral skeletons, *Nature*, *273*, 199–202.
- Evans, J. W. (1972), Tidal growth increments in the Cockle *Clinocardium nuttalli*, *Science*, *176*, 416–417.
- Feigl, F. (1958), *Spot Tests in Inorganic Analysis*, 5th ed., 600 pp., Elsevier, New York.
- Friedman, I., and J. R. O'Neil (1977), Compilation of stable isotope fractionation factors of geochemical interest, in *Data of Geochemistry*, edited by M. Fleischer, pp. 1–12, U.S. Govt. Print. Office, Washington, D. C.
- Fry, B. (2002), Conservative mixing of stable isotopes across estuarine salinity gradients: A conceptual framework for monitoring watershed influences on downstream fisheries production, *Estuaries*, *25*, 264–271.
- Gonfiantini, R., W. Stichler, and K. Rozanski (1995), Standards and intercomparison materials distributed by the International Atomic Energy Agency for stable isotope measurements, in *References and Intercomparison Materials for Stable Isotopes of Light Elements*, edited by the Isotope Hydrology Section of the International Atomic Energy Agency, pp. 13–29, IAEA, Vienna, Austria.
- Goodwin, D. H., K. W. Flessa, B. R. Schöne, and D. L. Dettman (2001), Cross-calibration of daily growth increments, stable isotope variation, and temperature in the Gulf of California

- bivalve mollusk *Chione cortezi*: Implications for paleoenvironmental analysis, *Palaios*, 16, 387–398.
- Goodwin, D. H., B. R. Schöne, and D. L. Dettman (2003), Resolution and fidelity of oxygen isotopes as paleotemperature proxies in bivalve mollusk shells: Models and observations, *Palaios*, 18, 110–125.
- Gordon, J., and M. R. Carriker (1978), Growth lines in a bivalve mollusk: Subdaily patterns and dissolution of the shell, *Science*, 202, 519–521.
- Grossman, E. L., and T. Ku (1986), Oxygen and carbon isotope fractionation in biogenic aragonite: Temperature effects, *Chem. Geol.*, 59, 59–74.
- Hays, J. D., J. Imbrie, and N. J. Shackleton (1976), Variation in the Earth's orbit: Pacemaker of the Ice Ages, *Science*, 194, 1121–1132.
- Hickson, J., A. L. A. Johnson, T. H. E. Heaton, and P. S. Balson (1999), The shell of the Queen Scallop *Aequipecten opercularis* (L.) as a promising tool for palaeoenvironmental reconstruction: Evidence and reasons for equilibrium stable-isotope incorporation, *Palaeogeogr. Palaeoclimatol. Palaeoecol.*, 154, 325–337.
- Huntley, B., and I. C. Prentice (1988), Temperatures in Europe from pollen data, 6000 years before present, *Science*, 241, 687–690.
- Jenkins, S. R., and R. G. Hartnoll (2001), Food supply, grazing activity, and growth rate in the limpet *Patella vulgata* L.: A comparison between exposed and sheltered shores, *J. Exp. Mar. Biol. Ecol.*, 258, 123–139.
- Jones, D. S. (1980), Annual cycle of shell growth increment formation in two continental shelf bivalves and its paleoecological significance, *Paleobiology*, 6, 331–340.
- Jones, D. S. (1983), Sclerochronology: Reading the record of the molluscan shell, *Am. Sci.*, 71, 384–391.
- Jones, D. S., and I. R. Quitmyer (1996), Marking time with bivalve shells: Oxygen isotopes and season of annual increment formation, *Palaios*, 11, 340–346.
- Jones, D. S., D. F. Williams, M. A. Arthur, and D. E. Krantz (1984), Interpreting the paleoenvironmental, paleoclimatic, and life history records in mollusc shells, *Geobios Mem. Spec.*, 8, 333–339.
- Jones, D. S., D. F. Williams, and C. S. Romanek (1986), Life history of symbiont-bearing giant clams from stable isotope profiles, *Science*, 231, 46–48.
- Jones, D. S., M. A. Arthur, and D. J. Allard (1989), Sclerochronological records of temperature and growth from shells of *Mercenaria mercenaria* from Narragansett Bay, Rhode Island, *Mar. Biol.*, 102, 225–234.
- Jones, D. S., I. R. Quitmyer, W. S. Arnold, and D. C. Marelli (1990), Annual shell banding, age, and growth rate of hard clams (*Mercenaria* spp.) from Florida, *J. Shellfish Res.*, 9, 215–225.
- Killingley, J. S., and W. A. Newman (1982), ^{18}O fractionation in barnacle calcite: A barnacle paleotemperature equation, *J. Mar. Res.*, 40, 893–902.
- Kim, S., and J. R. O'Neil (1997), Equilibrium and nonequilibrium oxygen isotope effects in synthetic carbonates, *Geochim. Cosmochim. Acta*, 61(16), 3461–3475.
- Klein, R. T., K. C. Lohmann, and C. W. Thayer (1996), Sr/Ca and $^{13}\text{C}/^{12}\text{C}$ ratios in skeletal calcite of *Mytilus trossulus*: Covariation with metabolic rate, salinity, and carbon isotopic composition of seawater, *Geochim. Cosmochim. Acta*, 60, 4207–4221.
- Krantz, D. E., D. F. Williams, and D. S. Jones (1987), Ecological and paleoenvironmental information using stable isotope profiles from living and fossil molluscs, *Palaeogeogr. Palaeoclimatol. Palaeoecol.*, 58, 249–266.
- Land, L. S., J. C. Lang, and D. J. Barnes (1977), On the stable carbon and oxygen isotopic composition of some shallow water, ahermatypic, scleractinian coral skeletons, *Geochim. Cosmochim. Acta*, 41, 169–172.
- Lewis, J. R., and R. S. Bowman (1975), Local habitat-induced variations in the population dynamics of *Patella vulgata* L., *J. Exp. Mar. Biol. Ecol.*, 17, 165–203.
- Lorrain, A., Y. Paulet, L. Chauvaud, R. Dunbar, D. Mucciarone, and M. Fontugne (2004), $\delta^{13}\text{C}$ variation in scallop shells: Increasing metabolic carbon contribution with body size?, *Geochim. Cosmochim. Acta*, 68, 3509–3519.
- Lowell, R. B. (1984), Desiccation of intertidal limpets: Effects of shell size, fit to substratum, and shape, *J. Exp. Mar. Biol. Ecol.*, 77, 197–207.
- Lutz, R. A., and D. C. Rhoads (1977), Anaerobiosis and a theory of growth line formation, *Science*, 198, 1222–1227.
- MacClintock, C. (1967), Shell structure of Patelloid and Bellerophonoid gastropods (Mollusca), *Peabody Mus. Nat. History Bull.*, 22, 140 pp.
- McConnaughey, T. (1989a), ^{13}C and ^{18}O isotopic disequilibrium in biological carbonates: Patterns, I, *Geochim. Cosmochim. Acta*, 53, 151–162.
- McConnaughey, T. (1989b), ^{13}C and ^{18}O isotopic disequilibrium in biological carbonates: II. In vitro simulation of kinetic isotope effects, *Geochim. Cosmochim. Acta*, 53, 163–171.
- McCrea, J. M. (1950), On the isotopic chemistry of carbonates and a paleotemperature scale, *J. Chem. Phys.*, 18, 849–857.
- McManus, J. F., G. C. Bond, W. S. Broecker, S. Johnsen, L. Labeyrie, and S. Higgins (1994), High-resolution climate records from the North Atlantic during the last interglacial, *Nature*, 371, 326–329.
- Oeschger, H., J. Beer, U. Siegenthaler, and B. Stauffer (1984), Late glacial climate history from ice cores, *Geophys. Monogr.*, 29, 299–306.
- Pannella, G. (1980), Growth patterns in fish sagittae, in *Skeletal Growth of Aquatic Organisms: Biological Records of Environmental Change*, edited by D. C. Rhoads and R. A. Lutz, pp. 469–491, Springer, New York.
- Pannella, G., and C. MacClintock (1968), Biological and environmental rhythms reflected in molluscan shell growth, in *Paleobiological Aspects of Growth and Development, A Symposium, Paleontol. Soc. Mem.*, vol. 2, edited by D. B. Macurda, *J. Paleontol.*, suppl., 42(5), 64–80.
- Prothero, D. R., and F. Schwab (1996), *Sedimentary Geology: An Introduction to Sedimentary Rocks and Stratigraphy*, 1st ed., 575 pp., W. H. Freeman, New York.
- Richardson, C. A., D. J. Crisp, and N. W. Runham (1979), Tidally deposited growth bands in the shell of the common cockle *Cerastoderma edule* (L.), *Malacologia*, 18, 277–290.
- Santina, P. D., E. Naylor, and G. Chelazzi (1994), Long term field actography to assess the timing of foraging excursions in the limpet *Patella vulgata* L., *J. Exp. Mar. Biol. Ecol.*, 178, 193–203.
- Schifano, G., and P. Censi (1983), Oxygen isotope composition and rate of growth of *Patella coerulea*, *Monodonta turbinata* and *M. articulata* shells from the western coast of Sicily, *Palaeogeogr. Palaeoclimatol. Palaeoecol.*, 42, 305–311.
- Schifano, G., and P. Censi (1986), Oxygen and carbon isotope composition, magnesium and strontium contents of calcite from a subtidal *Patella coerulea* shell, *Chem. Geol.*, 58, 325–331.
- Schöne, B. R., and D. Surge (Eds.) (2005), Special issue: Looking back over skeletal diaries—High-resolution environmental reconstructions from accretionary hard parts of

- aquatic organisms, *Palaeogeogr. Palaeoclimatol. Palaeoecol.*, **228**, 191 pp.
- Schöne, B. R., J. Lega, K. W. Flessa, D. H. Goodwin, and D. L. Dettman (2002), Reconstructing daily temperatures from growth rates of the intertidal bivalve mollusk *Chione cortezi* (northern Gulf of California, Mexico), *Palaeogeogr. Palaeoclimatol. Palaeoecol.*, **184**, 131–146.
- Schöne, B. R., E. Dunca, J. Fiebig, and M. Pfeiffer (2005a), Mutvei's solution: An ideal agent for resolving microgrowth structures of biogenic carbonates, *Palaeogeogr. Palaeoclimatol. Palaeoecol.*, **228**, 149–166.
- Schöne, B. R., S. D. Houk, A. D. Freyre Castro, J. Fiebig, W. Oschmann, I. Kröncke, W. Dreyer, and F. Gosselck (2005b), Daily growth rates in shells of *Arctica islandica*: Assessing sub-seasonal environmental controls on a long-lived bivalve mollusk, *Palaaios*, **20**, 78–92.
- Schöne, B. R., D. L. Rodland, A. Wehrmann, B. Heidel, W. Oschmann, Z. Zhang, J. Fiebig, and L. Beck (2007), Combined sclerochronologic and oxygen isotope analysis of gastropod shells (*Gibbula cineraria*, North Sea): Life-history traits and utility as a high-resolution environmental archive for kelp forests, *Mar. Biol.*, **150**(6), 1237–1252, doi:10.1007/s002270060435.
- Shackleton, N. J. (1973), Oxygen isotope analysis as a means of determining season of occupation of prehistoric midden sites, *Archaeometry*, **15**, 133–141.
- Signor, P. W. (1982), Growth-related surficial resorption of the penultimate whorl in *Terebra dimidiata* (Linnaeus, 1758) and other marine prosobranch gastropods, *Veliger*, **25**, 79–82.
- Smith, H. S., M. Delafontaine, and B. W. Flemming (1988), Intertidal barnacles—Assessment of their use as paleo-environment indicators using Mg, Sr, ¹⁸O/¹⁶O and ¹³C/¹²C variations, *Chem. Geol.*, **73**, 211–220.
- Smith, J. E., H. P. Schwarcz, M. J. Risk, T. A. McConnaughey, and N. Keller (2000), Paleotemperatures from deep-sea corals: Overcoming “vital effects”, *Palaaios*, **15**, 25–32.
- Spero, H. J., and D. W. Lea (1996), Experimental determination of stable isotope variability in *Globigerina bulloides*: Implications for paleoceanographic reconstructions, *Mar. Microorg.*, **28**, 231–246.
- Spero, H. J., J. Bijma, D. W. Lea, and B. E. Bemis (1997), Effect of seawater carbonate concentration on foraminiferal carbon and oxygen isotopes, *Nature*, **390**, 497–500.
- Surge, D., and K. J. Walker (2006), Geochemical variation in microstructural shell layers of the southern quahog (*Merccenaria campechiensis*): Implications for reconstructing seasonality, *Palaeogeogr. Palaeoclimatol. Palaeoecol.*, **237**, 182–190.
- Surge, D., K. C. Lohmann, and D. L. Dettman (2001), Controls on the isotopic chemistry of the American oyster, *Crassostrea virginica*: Implications for growth patterns, *Palaeogeogr. Palaeoclimatol. Palaeoecol.*, **172**, 283–296.
- Surge, D. M., K. C. Lohmann, and G. A. Goodfriend (2003), Reconstructing estuarine conditions: Oyster shells as recorders of environmental change, southwest Florida, *Estuarine Coastal Shelf Sci.*, **57**, 737–756.
- Swart, P. K. (1983), Carbon and oxygen isotope fractionation in scleractinian corals: A review, *Earth Sci. Rev.*, **19**, 51–80.
- Tarutani, T., R. N. Clayton, and T. K. Mayeda (1969), The effect of polymorphism and magnesium substitution on oxygen isotope fractionation between calcium carbonate and water, *Geochim. Cosmochim. Acta*, **33**, 987–996.
- Urdowski, E., and J. Hoefs (1993), Oxygen isotope exchange between carbonic acid, bicarbonate, carbonate, and water: A re-examination of the data of McCrea [1950] and an expression for the overall partitioning of oxygen isotopes between the carbonate species and water, *Geochim. Cosmochim. Acta*, **57**, 3815–3818.
- Verderber, G. W., S. B. Cook, and C. B. Cook (1982), The role of the home scar in reducing water loss during aerial exposure of the pulmonate limpet, *Siphonaria alternata* (Say), *Veliger*, **25**, 235–243.
- Walker, K. J., and D. Surge (2006), Developing oxygen isotope proxies from archaeological sources for the study of Late Holocene human-climate interactions in coastal southwest Florida, *Quat. Int.*, **150**, 3–11.
- Wang, Y., and W. Tzeng (1999), Differences in growth rates among cohorts of *Encrasicholina punctifer* and *Engraulis japonicus* larvae in the coastal waters off Tanshui River Estuary, Taiwan, as indicated by otolith microstructure analysis, *J. Fish Biol.*, **54**, 1002–1016.
- Wefer, G., and W. H. Berger (1980), Stable isotopes in benthic foraminifera: Seasonal variation in large tropical species, *Science*, **209**, 803–805.
- Wefer, G., and W. H. Berger (1981), Stable isotope composition of benthic calcareous algae from Bermuda, *J. Sediment. Petrol.*, **51**, 459–465.
- Wefer, G., and W. H. Berger (1991), Isotope paleontology: Growth and composition of extant calcareous species, *Mar. Geol.*, **100**, 207–248.
- Wefer, G., and J. S. Killingley (1980), Growth histories of Strombid snails from Bermuda recorded in their O-18 and C-13 profiles, *Mar. Biol.*, **60**, 129–135.
- Weidman, C. R., G. A. Jones, and K. C. Lohmann (1994), The long-lived mollusk *Arctica islandica*: A new paleoceanographic tool for the reconstruction of bottom temperatures for the continental shelves of the northern North Atlantic Ocean, *J. Geophys. Res.*, **99**, 18,305–18,314.
- Wheeler, A. P. (1992), Mechanisms of molluscan shell formation, in *Calcification in Biological Systems*, edited by E. Bonucci, pp. 179–216, CRC Press, Boca Raton, Fla.
- Williams, D. F., M. A. Arthur, D. S. Jones, and N. Healy-Williams (1982), Seasonality and mean annual sea surface temperatures from isotopic and sclerochronological records, *Nature*, **296**, 432–434.
- Zeebe, R. E. (1999), An explanation of the effect of seawater carbonate concentration on foraminiferal oxygen isotopes, *Geochim. Cosmochim. Acta*, **63**, 2001–2007.